Journal of Macromolecular Science, Part A
Publication details, including instructions for authors and subscription information:
http://www.informaworld.com/smpp/title~content=t713597274

Comparison of Singlet Oxygen Generation Efficiency between Water-Soluble C_{60}-Diphenylaminofluorene Conjugates and Molecular Micelle-like FC_4S

Grace So[ab]; Aliaksandr Karotki[c]; Sarika Verma[d]; Kenneth Pritzker[b]; Brian Wilson[c]; Long Y. Chiang[d]
[a] Department of Materials Science and Engineering, University of Toronto, Toronto, Canada [b] Department of Pathology and Laboratory Medicine, Mount Sinai Hospital and University of Toronto, Toronto, Canada [c] Ontario Cancer Institute, University Health Network, Toronto, Canada [d] Department of Chemistry, University of Massachusetts Lowell, Lowell, MA

To cite this Article So, Grace , Karotki, Aliaksandr , Verma, Sarika , Pritzker, Kenneth , Wilson, Brian and Chiang, Long Y.(2006) 'Comparison of Singlet Oxygen Generation Efficiency between Water-Soluble C_{60}-Diphenylaminofluorene Conjugates and Molecular Micelle-like FC_4S', Journal of Macromolecular Science, Part A, 43: 12, 1955 — 1963
To link to this Article: DOI: 10.1080/10916460600997629
URL: http://dx.doi.org/10.1080/10916460600997629

Journal of Macromolecular Science®, Part A: Pure and Applied Chemistry, 43:1955–1963, 2006

ISSN 1060-1325 print/1520-5738 online
DOI: 10.1080/10916460600997629

Comparison of Singlet Oxygen Generation Efficiency between Water-Soluble C_{60}-Diphenylaminofluorene Conjugates and Molecular Micelle-like FC_4S

GRACE SO,[1,2] ALIAKSANDR KAROTKI,[3] SARIKA VERMA,[4] KENNETH PRITZKER,[2] BRIAN WILSON,[3] AND LONG Y. CHIANG[4]

[1]Department of Materials Science and Engineering, University of Toronto, Toronto, Canada
[2]Department of Pathology and Laboratory Medicine, Mount Sinai Hospital and University of Toronto, Toronto, Canada
[3]Ontario Cancer Institute, University Health Network, Toronto, Canada
[4]Department of Chemistry, University of Massachusetts Lowell, Lowell, MA

Amphiphilic C_{60}-diphenylaminofluorene conjugates C_{60} (>DPAF-EG_n) exhibit good water-solubility and form self-assembled bilayer vesicles in dilute aqueous solution. Their singlet oxygen generation efficiency in DMF or H_2O was evaluated by using time-resolved measurements of singlet oxygen luminescence at 1270 nm upon photoexcitation by nanosecond pulse laser operated at 523 nm. By the application of different bandpass filters to cut off certain emission at wavelength ranges outside 1270 nm, a distinguishable peak in medium to high integrated luminescence intensity was collected at wavelengths between 1240 and 1300 nm. It provided confirmation and close correlation of emitted photon counts measured for these fullerene derivatives to singlet oxygen. In contrast to apparently high singlet oxygen generation efficiency of FC_4S in H_2O, an observed low singlet oxygen production rate from aqueous solutions of C_{60} (>DPAF-EG_{14}) and C_{60} (>DPAF-EG_{45}) was interpreted as the result of the occurrence of competitive ultrafast intramolecular electron transfer going from DPAF moiety to C_{60} cage moiety. That eliminated largely the possibility of energy transfer process for fullerenyl intersystem crossing to generate $^3C_{60}^*$(>DPAF-EG_n). Instead, radical ion-pairs containing molecules $C_{60}^{-\cdot}$ [>(DPAF-EG_n)$^{+\cdot}$] were produced via the intramolecular electron transfer process in the photoexcited transient state.

Keywords photodynamic therapy, fullerenes, cell toxicity, singlet oxygen

Introduction

Spherical fullerenes are molecules composed of a stable 3D closed cage structure with reactive (6,6]olefinyl double bonds capable of undergoing chemical functionalization,

Address correspondence to Long Y. Chiang, Department of Chemistry, University of Massachusetts Lowell, Lowell, MA 01854. E-mail: long_chiang@uml.edu and Kenneth Pritzker, Department of Pathology and Laboratory Medicine, Mount Sinai Hospital and University of Toronto, Toronto, Canada. E-mail: kpritzker@mtsinai.on.ca

leading to derivatives with one or multiple attachments of organic groups on the cage. Fullerene cage is highly hydrophobic. Various degrees of hydrophilicity can be introduced via functionalization with polar attachments. Increased hydrophilicity of fullerene derivatives makes them suitable as electronic or photonic agents in potential material applications related to biomedical science (1, 2). One area of hydrophilic fullerene applications was demonstrated by photodynamic therapy (PDT) for tumor or cancer treatments (3). Success of the PDT approach arises from its highly targeted local therapeutic method that uses a combination of photosensitizing drugs and non-thermal laser radiation to produce cytotoxic effect on the cells (4, 5). In the practice of hydrophilic fullerene drugs, they were normally administered intravenously or topically. After a bio-distribution period of 24 h for the drug to accumulate at the targeted tissue site, it was irradiated with a laser light source in a defined light dose. That induced the excitation of fullerenyl photosensitizer to its excited singlet state. Subsequent intersystem energy crossing going from the excited singlet state to triplet state occurred in a nearly quantitative yield for the C_{60} cage, giving the corresponding triplet $^3C_{60}^*$ moiety. Triplet energy transfer from $^3C_{60}^*$ to molecular oxygen ($^3O_2$) is an efficient process and produces reactive singlet oxygen species ($^1O_2$) (6, 7). Singlet oxygen is very reactive and causes either oxidative damage to surrounding biological molecules or induces irreversible biological responses that destroy the targeted tissue in the effect of photocytotoxicity(3, 8).

In general, derivatives of highly functionalized C_{60} with more than 6 hydrophilic arm attachments are not toxic to biological subjects without extensive photoactivation (9). However, photodynamic efficiency and the quantum yield of singlet oxygen generation may decrease significantly upon chemical modifications of C_{60}. Examples were given by malonic acid derivatives of fullerene $C_{60}[>(COOR)_2]_n$, where R is either H or Et and $n = 1 - 6$, with sharply declined fullerenyl triplet state properties as n approaches 3 or higher (10). Quantum yield of singlet oxygen generation becomes negligible for the fully symmetrical yellow hexaadduct molecule $C_{60}[>(COOEt)_2]_6$. Recently, we demonstrated highly photodynamic, water-soluble C_{60} hexaadduct hexa(sulfo-*n*-butyl)[60]fullerenes, FC_4S, with retention of excellent singlet oxygen production efficiency(7). That made FC_4S a very promising candidate as a photosensitizer for PDT treatments(3).

Another class of water-soluble fullerene derivatives were developed to incorporate a photoresponsive chromophore directly bound on the C_{60} cage for light harvesting and poly(ethylene oxide) chains for hydrophilicity. That led to oligo(ethylene glycolated) diphenylaminofluoreno-carbonyl-methano[60]fullerene, $C_{60}(>\text{DPAF-EG}_{14})$ and $C_{60}(>\text{DPAF-EG}_{45})$ (11), as shown in Figure 1. In this paper, we evaluated the singlet oxygen generation efficiency of $C_{60}(>\text{DPAF-EG}_{14})$ and $C_{60}(>\text{DPAF-EG}_{45})$ in water with the value compared with that of molecular micelle-like FC_4S.

Experimental

General and Materials Preparation

Synthesis of FC_4S was described previously by Chiang, et al. (12). Experimental procedures for the synthesis of $C_{60}(>\text{DPAF-EG}_{14})$ and $C_{60}(>\text{DPAF-EG}_{45})$ were reported recently (11, 13). Two poly(ethylene glycol) bis(carboxymethyl)ether samples in a molecular weight of 600 and 2,000 were purchased from Aldrich and used in the esterification reaction with C_{60}-methanocarbonyl-9,9-dihydroxyethan-2-diphenylaminofluorene, $C_{60}(>\text{DPAF-OH})$, to afford the corresponding C_{60}-methanocarbonyl-9,9-

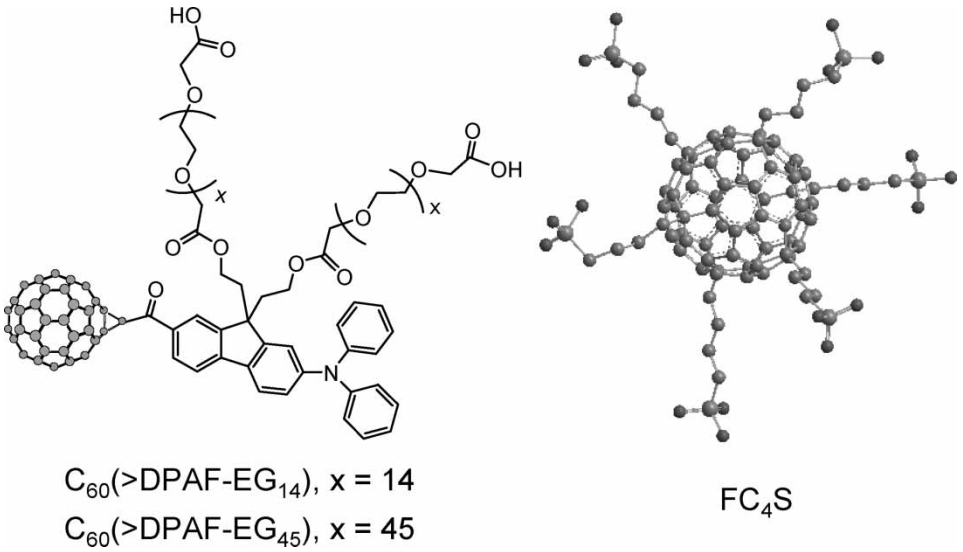

Figure 1. Molecular structures of C_{60}(>DPAF-EG_{14}) (M.W. of PEG chains as 600), C_{60}(>DPAF-EG_{45}) (M.W. of PEG chains as 2000), and $C_{60}(CH_2CH_2CH_2CH_2SO_3Na)_6$ (FC_4S, schematic representation based on a symmetrical analogous of the isomers).

dioligoethyleneglycol-2-diphenylaminofluorenes C_{60}(>DPAF-EG_{14}) and C_{60}(>DPAF-EG_{45}), respectively. Both structures of water-soluble C_{60}-DPAF conjugates were purified on thin layer chromatography and subsequently characterized and confirmed by infrared, UV-Vis, ^{1}H-NMR, and ^{13}C-NMR spectroscopy recorded on a Nicolet 750 series FT-IR, Perkin-Elmer UV/VIS/NIR Lambda 9 series, and a Bruker Spectrospin−250 spectrometers, respectively.

Measurements of Singlet Oxygen Generation

Measurements of time-resolved singlet oxygen ($^1O_2$) signal intensity were performed by making direct correlation to the detection of its near-IR luminescence at 1270 nm corresponding to the emission of $^1O_2$ at $^1\Delta_g \rightarrow {}^3\Sigma_g^-$ transition. Detailed experimental setup was described in previous report(14). All measurements were carried with C_{60}-DPAF conjugates in a concentration of either 10 μM or 50 μM. In a general procedure, hydrophilic fullerene derivatives were dissolved in the solvent and photoexcited by a frequency-doubled Nd:YAG laser (QG-523-500, Crystalaser Inc., Reno, NV) at 523 nm. The pulse duration and pulse repetition rate were 10 ns and approximately 3 kHz, respectively. Luminescence emitted from singlet oxygen was detected by a PMT detector (R5509-42, Hamamatsu Corp., Bridgewater, NJ) with high sensitivity in the near-IR region. Five bandpass filters, each with a cut-off wavelength at 1210 nm, 1240 nm, 1270 nm, 1300 nm, or 1330 nm, were placed sequentially in front of the photodetector to allow sampling of the corresponding range of luminescence spectrum. Time-resolved kinetics of singlet oxygen luminescence, $S(t)$, were fitted with the following Equation (1) (14):

$$S(t) = C[\exp(-t/\tau_T) - \exp(-t/\tau_\Delta)] \quad (1)$$

where C is a constant, τ_T and τ_Δ are triplet state and singlet oxygen lifetime, respectively.

Results and Discussion

Attachment of two oligo(ethylene glycol) groups (EG_n), in a molecular weight of either 600 and 2,000, to C_9 position of the fluorene ring of DPAF moiety significantly increases the water-solubility of corresponding conjugate derivatives diphenylaminofluoreno-carbonyl-methano[60]fullerenes, C_{60}(>DPAF-EG_{14}) and C_{60}(>DPAF-EG_{45}), respectively. In this structure, the C_{60} cage and diphenylaminofluorene moieties remain highly hydrophobic and not compatible with H_2O. This large difference in hydrophobicity and hydrophilicity of separate molecular components in a joint compound forces the water-insoluble C_{60}-DPAF component to pack with the same component of different molecules in aqueous solution into coalesce nanoparticles, while water-soluble oligo(ethylene glycol) groups bound on the same molecules give high tendency of dispersion into the aqueous phase. That resulted in distinguishable molecular self-assembly behaviors of amphiphilic C_{60}(>DPAF-EG_n) in H_2O. For example, studies under transmission electron microscopy (TEM) and dynamic light scattering (DLS) measurements evidently substantiated the nano- to submicron-sized spherical vesicle formation in the solution of C_{60}(>DPAF-EG_{14}) in various concentrations ranging from 3.0×10^{-3} to 1.0×10^{-6} M (11). Small-sized nanoparticles were found in a diameter of 60–100 nm in a mixture of large-sized vesicles in a range of 200–450 nm. Interestingly, relatively large oligo(ethylene glycol) groups prohibited multilayers aggregation of C_{60}(>DPAF-EG_{14}) to incorporate water-soluble EG_n components deep inside the phase-separated particle. Accordingly, molecular packing of C_{60}(>DPAF-EG_{14}) settled in arrangement of a bilayer structure. This type of C_{60}-derived vesicles may serve as an alternative to lipid membranes and liposome vesicles. As the chain length of EG_n increases to 2000 in chain weight as that in the structure of C_{60}(>DPAF-EG_{45}), many small-sized vesicles in an average size of less than ~60 nm in diameter becomes possible. These nanostructures in aqueous solution were used in this study.

UV-Vis absorption spectra of C_{60}(>DPAF-EG_{14}), C_{60}(>DPAF-EG_{45}), and FC_4S were recorded in water and normalized to the absorption peak at 300 nm, as shown in Figure 2. In the case of FC_4S, the main optical absorption occurred at the wavelength

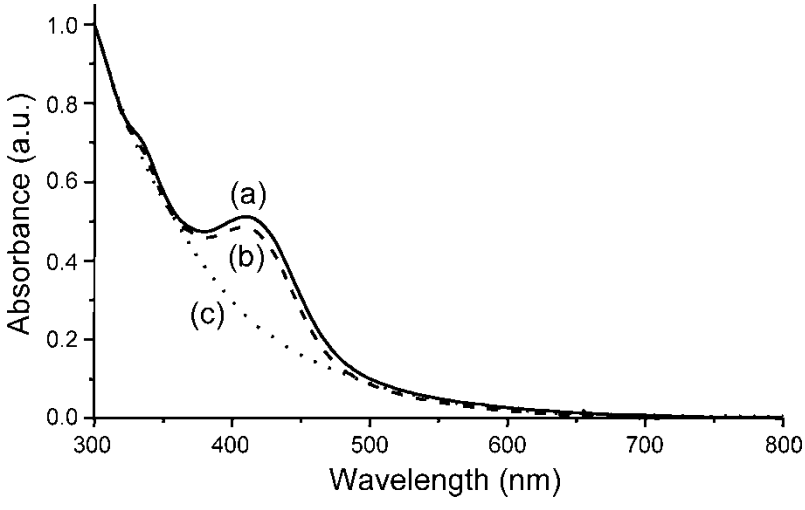

Figure 2. Steady state absorption spectra of (a) C_{60}(>DPAF-EG_{14}), (b) C_{60}(>DPAF-EG_{45}), and (c) FC_4S in water normalized to the absorbance maximum at 300 nm.

range below 350 nm with a shoulder extending to beyond 650 nm. An additional band centered at 425 nm for C_{60}(>DPAF-EG_{14}) and C_{60}(>DPAF-EG_{45}) was assigned to the characteristic optical absorption of DPAF chromophore (15). It was also accompanied with a shoulder extending to beyond 650 nm. That makes these two C_{60}-DPAF derivatives and FC_4S photoresponsive to nearly all visible wavelengths in aqueous solution.

It is generally recognized that the presence of reactive oxygen species (ROS), including singlet oxygen ($^1O_2$), hydroxyl radical (OH·), and superoxide radical (O_2^-·), becomes the main toxin source giving rise to the damage of the cell and tissue. Previous observation of high efficiency in the generation of singlet oxygen by FC_4S in water upon laser light exposure at 400–630 nm allowed its uses as cytotoxic photosensitizers in photodynamic therapy against tumors and cancers (3). This phenomenon is associated with photoexcitation of FC_4S molecules to its singlet excited state $^1FC_4S^*$ followed by the intersystem crossing of singlet excited energy into its triplet excited state $^3FC_4S^*$. Singlet oxygen is then produced by subsequent energy transfer from $^3FC_4S^*$ to surrounding oxygen molecules ($^3O_2$) at the ground state. Since FC_4S was proven to be highly effective for both *in vitro* and *in vivo* PDT treatments using fibrosarcoma cells as a model(3), its singlet oxygen production data can be applied as a reference for comparison with that of C_{60}(>DPAF-EG_n) compounds in this study.

The best method to evaluate the singlet oxygen generation efficiency is to detect directly the fluorescence emission of singlet oxygen at 1270 nm. It was carried out by using a frequency-doubled Nd:YAG laser operated at 523 nm with a pulse duration of 10 ns as the light source to activate C_{60}(>DPAF-EG_n) molecules. Subsequent luminescence from the solution was collected by a photodetector with the photon counted in a time-resolved manner up to 200 μs after pulse photoexcitation. Results of C_{60}(>DPAF-EG_{14}) and C_{60}(>DPAF-EG_{45}) in dimethylformamide were depicted in Figure 3 showing a detectable intensity of singlet oxygen luminescence with monotonic decay in a normal kinetic rate up to 50 μs without a long tail. Data fitting of the decay profile using Equation (1) resulted in singlet oxygen lifetimes equal to 11.9 μs for C_{60}(>DPAF-EG_{14}) and 10.8 μs for C_{60}(>DPAF-EG_{45}) in values slightly lower than that reported for FC_4S

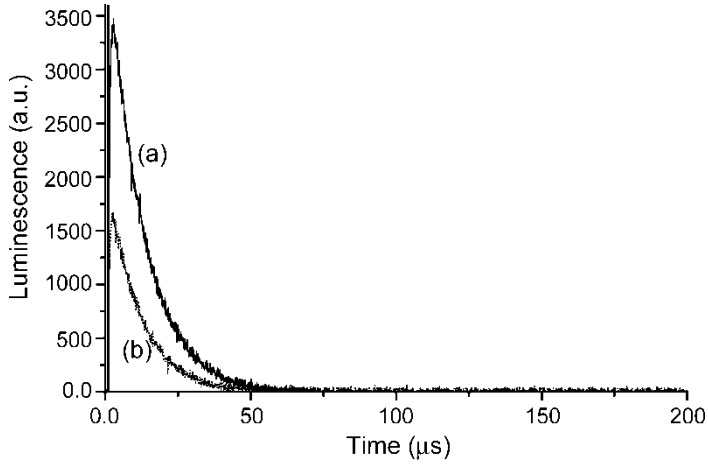

Figure 3. Time-resolved singlet oxygen luminescence emission of (a) C_{60}(>DPAF-EG_{14}) and (b) C_{60}(>DPAF-EG_{45}) in DMF in a concentration of 50 μM.

(17.9 μs) (7) and literature values in DMF (16, 17). Observation substantiated the capability of C_{60}(>DPAF-EG_n) analogous amphiphilic molecules in the production of $^1O_2$ in DMF.

Similar time-resolved measurements were performed in H_2O, where the bilayer vesicle formation is likely for C_{60}(>DPAF-EG_n) conjugates. It is worthwhile to note that the maximum $^1O_2$ luminescence emission decreases significantly in aqueous solution from that in DMF by taking relatively short $^1O_2$ lifetime (18, 19) in H_2O into account. However, there was no difficulty in detecting good intensity of singlet oxygen luminescence from aqueous solution of FC_4S upon photoexcitation at 523 nm, as shown in Figure 4. Fitting of this curve with Equation (1) led to the singlet oxygen lifetime value of 3.8 μs in water in approximately good agreement with the literature data (18). Quantum yield $\Phi(^1O_2)$ of FC_4S in the generation of $^1O_2$ was roughly estimated previously to be 0.36 with the pseudo-first-order triplet-quenching rate constant of $1.28 \times 10^9\ M^{-1}\ s^{-1}$ (7), by the direct comparison of its luminescence emission characteristics produced from γ-cyclodextrin encapsulated C_{60} (C_{60}/γ-CD) in water giving $\Phi(^1O_2)$ as 0.98 (20). Amplitude of singlet oxygen luminescence signals produced by C_{60}(>DPAF-EG_{14}) and C_{60}(>DPAF-EG_{45}) was clearly much smaller than that for FC_4S, indicating much more singlet oxygen generated by the latter. Signal profiles in a short microsecond region of less than 15 μs and the shape of extended luminescence curve in a long microsecond region up to 50 μs, showing long, non-monoexponential decay, were also qualitatively different from those of FC_4S.

A secondary time-resolved measurement was made by integrating singlet oxygen luminescence intensity produced from C_{60}(>DPAF-EG_{14}), C_{60}(>DPAF-EG_{45}), and FC_4S in aqueous solution immediately after nanosecond laser photoexcitation at 523 nm. The measurement was coupled with the placement of five different bandpass filters, each with a cut-off wavelength at 1210 nm, 1240 nm, 1270 nm, 1300 nm, or 1330 nm, sequentially in front of the photodetector to collect the luminescence emission spectrum in the corresponding defined wavelength region. The plots were

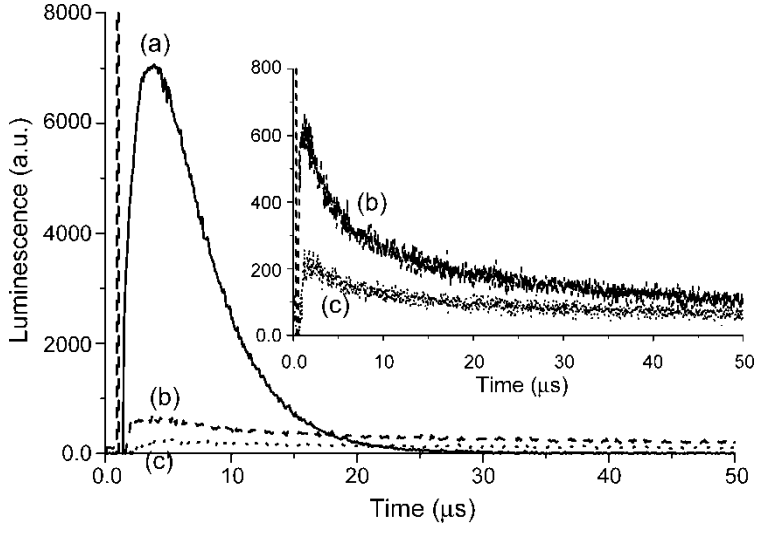

Figure 4. Time-resolved singlet oxygen luminescence emission of (a) FC_4S, (b) C_{60}(>DPAF-EG_{14}), and (c) C_{60}(>DPAF-EG_{45}) in H_2O. The insert shows the data over a longer time scale. All measurements were made in 10 μM solutions with 523 nm excitation.

depicted in Figure 5 showing a sharp increase in intensity of the luminescence peak at 1270 nm for all water-soluble fullerene samples measured. The peak can be distinguished unambiguously from that collected at nearby wavelengths of 1240 and 1300 nm that provided confirmation of emitted photon counts measured from these hydrophilic fullerene solutions being correlated closely to singlet oxygen.

A marked difference in the observed singlet oxygen production efficiency between $C_{60}(>\text{DPAF-EG}_n)$ and FC_4S was interpreted as follows. Molecular micellar structure of FC_4S allowed molecular oxygen to diffuse very efficiently into self-assembled aggregates of FC_4S that consists of nearly monodisperse spheroidal nanospheres with the sphere radius of gyration $R_g \approx 19$ Å with the major axe ≈ 29 Å and the minor axe ≈ 21 Å for ellipsoid-like aggregates in H_2O. Long sphere diameter of this nanostructure was estimated to be 60 Å (21, 22). Based on the hydrodynamic volume of the sphere, a large number of H_2O molecules trapped inside the core of nanospheres was proposed that makes efficient molecular contact of O_2 with the C_{60} cage moiety to facilitate triplet energy transfer from $^3FC_4S^*$ to $^3O_2$. The phenomena led to consistent observation of high singlet oxygen luminescence emission of FC_4S.

In the case of $C_{60}(>\text{DPAF-EG}_n)$ molecules, formation of bilayer vesicles in H_2O was evident that may also provide easy access of molecular oxygen in aqueous phase to excited fullerene cage moieties in the membrane. The fact of their low singlet oxygen intensity detected in H_2O may be reasoned by the lack of excited triplet intermediates $^3C_{60}^*(>\text{DPAF-EG}_n)$ existing within the bilayer membrane of vesicles. The efficiency of intersystem energy crossing going from $^1C_{60}^*$ to $^3C_{60}^*$ is nearly quantitative, thus, a low concentration of $^3C_{60}^*(>\text{DPAF-EG}_n)$ should also correlate to the unfavorable formation of $^1C_{60}^*(>\text{DPAF-EG}_n)$ during photoexcitation at 523 nm. Evidently, optical absorption of DPAF moiety is much higher in intensity than C_{60} cage in the visible range of 480–550 nm. That allowed us to suggest that DPAF moiety was the main chromophore in response to photoexcitation at 523 nm and produced the corresponding excited $C_{60}[>{}^1(\text{DPAF-EG}_n)^*]$ intermediate. Based on recent nanosecond transient absorption measurements of $C_{60}(>\text{DPAF-EG}_{14})$ carried out by laser photolysis at 523 nm excitation in deaerated H_2O(11), no significant transient absorption of triplet $^3C_{60}^*$ state at 740 nm

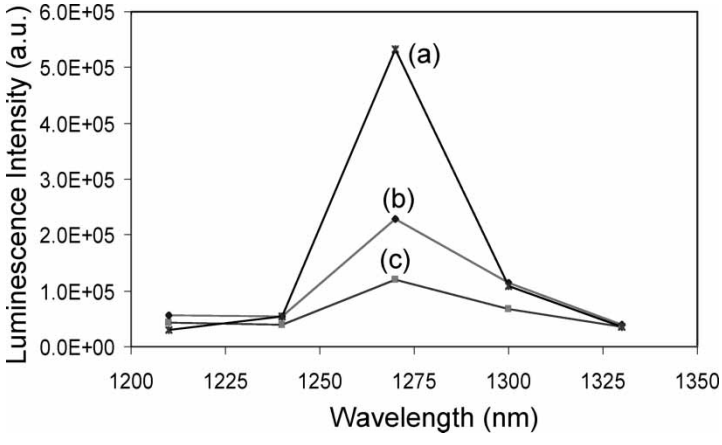

Figure 5. Integrated luminescence intensity of singlet oxygen produced from (a) FC_4S (b) C_{60} $(>\text{DPAF-EG}_{14})$, and (c) $C_{60}(>\text{DPAF-EG}_{45})$ in H_2O upon photoexcitation at 523 nm with the application of different bandpass filters.

was observed immediately after the laser pulse. It revealed little or no involvement of a fullerenyl triplet state during the photoexcitation process. Contrarily, two new transient absorption bands at 840 and 1000 nm were detected in 10 ns time scale. They were attributed to absorptions of the DPAF radical cation ($DPAF^{+}\cdot$) and the radical anion of C_{60} moiety ($C_{60}^{-}\cdot$), respectively, indicating clearly the intramolecular electron transfer and charge-separation process taking place via $C_{60}[>{}^{1}(DPAF\text{-}EG_n)^{*}]$. This competitive ultrafast intramolecular electron transfer from DPAF moiety to C_{60} cage moiety eliminated the possibility of energy transfer process for intersystem crossing. Therefore, a low singlet oxygen production rate from aqueous solutions of $C_{60}(>DPAF\text{-}EG_{14})$ and $C_{60}(>DPAF\text{-}EG_{45})$ was expected.

Conclusions

Singlet oxygen generation efficiency of $C_{60}(>DPAF\text{-}EG_{14})$ and $C_{60}(>DPAF\text{-}EG_{45})$ in DMF or H_2O upon photoexcitation by nanosecond pulse laser operated at 523 nm was evaluated and correlated by measurements of time-resolved luminescence kinetics at 1270 nm, corresponding to the fluorescence emission wavelength of singlet oxygen. By using different bandpass filters to cut off certain emission at wavelength ranges outside 1270 nm, a distinguishable peak in high integrated luminescence intensity was collected at wavelengths between 1240 and 1300 nm. It provided the confirmation of emitted photons from these hydrophilic fullerene derivatives being correlated closely to singlet oxygen. In contrast to apparently high singlet oxygen generation efficiency of FC_4S in H_2O, an observed low singlet oxygen production rate from aqueous solutions of $C_{60}(>DPAF\text{-}EG_{14})$ and $C_{60}(>DPAF\text{-}EG_{45})$ was interpreted as the result of the occurrence of competitive ultrafast intramolecular electron transfer from DPAF moiety to C_{60} cage moiety. That eliminated largely the possibility of energy transfer process for fullerenyl intersystem crossing to generate $^{3}C_{60}{}^{*}(>DPAF\text{-}EG_n)$. Instead, radical ion-pairs containing molecules $C_{60}^{-}\cdot[>(DPAF\text{-}EG_n)^{+}\cdot]$ were produced in the photoexcited transient state in H_2O.

Acknowledgements

The authors thank Mark Niedre for singlet oxygen measurement assistance and Jindra Tupy for lab assistance. Singlet oxygen measurements were supported by a grant of the National Cancer Institute of Canada. A. Karotki is supported by the Canadian Institute for Photonic Innovations. Synthesis of C_{60}-DPAF conjugates was supported by the Air Force Office of Scientific Research under contract number FA9550-05-1-0154.

References

1. Nierengarten, J.-F. (2004) *New J. Chem.*, 28: 1177–1191.
2. Bosi, S., Da Ros, T., Spalluto, G., and Prato, M. (2003) *Eur. J. Med. Chem.*, 38: 913–923.
3. Yu, C., Canteenwala, T., Chen, H.H.C., Chen, B.J., Canteenwala, M., and Chiang, L.Y. (1999) *Proc. Electrochem. Soc.*, 12: 234–249.
4. Dougherty, T.J., Gomer, C.J., Henderson, B.W., Jori, G., Kessel, D., Korbelik, M., Moan, J., and Peng, Q. (1998) *J. Natl. Cancer Inst.*, 90: 889–905.
5. Wilson, B.C. and Patterson, M.S. (1986) *Phys. Med. Biol.*, 31: 327–360.
6. Arbogast, J.W., Darmanyan, A.P., Foote, C.S., Rubin, Y., Diederich, F.N., Alvarez, M.M., Anz, S.J., and Whetten, R.L. (1991) *J. Am. Chem. Soc.*, 95: 11–12.

7. Yu, C., Canteenwala, T., El-Khouly, M.E., Araki, Y., Pritzker, K., Ito, O., Wilson, B.C., and Chiang, L.Y. (2005) *J. Mater. Chem.*, 15: 1857–1864.
8. Yang, X.L., Fan, C.H., and Zhu, H.S. (2002) *Toxic. in Vitro*, 16: 41–46.
9. Sayes, S.M., Fortner, J.D., Guo, W., Lyon, D., Boyd, A.M., Ausman, K.D., Tao, Y.J., Sitharaman, B., Wilson, L.J., Hughes, J.B., West, J.L., and Colvin, V.L. (2004) *Nano Lett.*, 4: 1881–1887.
10. Bensasson, R.V., Berberan-Santos, M.N., Brettreich, M., Frederiksen, J., Göttinger, H., Hirsch, A., Land, E.J., Leach, S., McGarvey, D.J., Schönberger, H., and Schröder, C. (2001) *Phys. Chem. Chem. Phys.*, 3: 4679–4683.
11. Verma, S., Hauck, T., El-Khouly, M.E., Padmawar, P.A., Canteenwala, T., Pritzker, K., Ito, O., and Chiang, L.Y. (2005) *Langmuir*, 21: 3267–3272.
12. Bhonsle, J.B., Yu, C., Huang, J.P., Shiea, J., Chen, B.J., and Chiang, L.Y. (1998) *Chem Lett.,* 465.
13. Verma, S., Padmawar, P.A., Hauck, T., Canteenwala, T., Chiang, L.Y., and Pritzker, K. (2005) *J. Macromol. Sci. A, Pure Appl. Chem.*, 42: 1497–1505.
14. Niedre, M., Paterson, M.S., and Wilson, B.C. (2002) *Photochem. Photobiol.*, 75: 382–391.
15. Padmawar, P.A., Canteenwala, T., Verma, S., Tan, L.-S., and Chiang, L.Y. (2004) *J. Macromol. Sci. A*, 41: 1387–1400.
16. Ogilby, P.R. and Sanetra, J. (1993) *J. Phys. Chem.*, 97: 4689.
17. Aveline, B., Delgado, O., and Brault, D. (1992) *J. Chem. Soc. Faraday Trans.*, 88: 1971.
18. Wilkinson, F., Helman, W.P., and Ross, A.B. (1995) *J. Phys. Chem. Ref. Data*, 24: 663–1021.
19. Patterson, M.S., Madsen, S.J., and Wilson, B. (1990) *J. Photochem. Photobiol. B*, 15: 69.
20. Konishi, T., Fujitsuka, M., Luo, H., Araki, Y., Ito, O., and Chiang, L.Y. (2003) *Fullerenes, Nanotubes and Carbon Nanostruct.*, 11: 237.
21. Jeng, U.S., Lin, T.L., Tsao, C.S., Lee, C.H., Canteenwala, T., Wang, L.Y., Chiang, L.Y., and Han, C.C. (1999) *J. Phys. Chem. B*, 103: 1059.
22. Liu, W.J., Jeng, U., Lin, T.L., Canteenwala, T., and Chiang, L.Y. (2001) *Fullerene Sci. Technol.*, 9: 131.